Spin-dependent electrical transport in ion-beam sputter deposited Fe-Cr multilayers

A. K. Majumdar*
Department of Physics, Indian Institute of Technology, Kanpur-208016, India
and Department of Physics, University of Florida, Gainesville, Florida 32611

A. F. Hebard
Department of Physics, University of Florida, Gainesville, Florida 32611

Avinash Singh
Department of Physics, Indian Institute of Technology, Kanpur-208016, India

D. Temple
MCNC, Electronics Technologies Division, Research Triangle Park, North Carolina 27709
(Received 19 August 2001; published 3 January 2002)

The temperature dependence of the electrical resistivity and magnetoresistance of Xe-ion-beam-sputtered Fe-Cr multilayers has been investigated. The electrical resistivity between 5 and 300 K in the fully ferromagnetic state, obtained by applying a field beyond the saturation field (H_{sat}) necessary for the antiferromagnetic- (AF-) ferromagnetic (FM) field-induced transition, shows evidence of spin-disorder resistivity as in crystalline Fe and an *s-d* scattering contribution (as in 3*d* metals and alloys). The sublattice magnetization $m(T)$ in these multilayers has been calculated in terms of the planar and interlayer exchange energies. The additional spin-dependent scattering $\Delta\rho(T)=\rho(T,H=0)_{AF}-\rho(T,H=H_{sat})_{FM}$ in the AF state over a wide range of temperature is found to be proportional to the sublattice magnetization, both $\Delta\rho(T)$ and $m(T)$ reducing along with the antiferromagnetic fraction. At intermediate fields, the spin-dependent part of the electrical resistivity $[\rho_s(T)]$ fits well to the power law $\rho_s(T)=b-cT^{\alpha}$ where c is a constant and b and α are functions of H. At low fields $\alpha\simeq 2$ and the intercept b decreases with H much the same way as the decrease of $\Delta\rho(T)$ with T. A phase diagram (T vs H_{sat}) is obtained for the field-induced AF-to-FM transition. Comparisons are made between the present investigation and similar studies using dc-magnetron-sputtered and molecular-beam-epitaxy-grown Fe-Cr multilayers.

DOI: 10.1103/PhysRevB.65.054408 PACS number(s): 75.50.Bb, 75.50.Ee, 72.15.Eb, 72.15.Gd

I. INTRODUCTION

As one of the very few lattice-matched transition-metal pairs one of which is ferromagnetic (FM), Fe-Cr multilayers offer excellent opportunities for investigating the exchange coupling of Fe layers through an antiferromagnetic Cr spacer layer, giving rise to the so-called giant magnetoresistance (GMR). Applications as magnetic-field sensors, especially in reading information, sensing position and speed of moving parts, etc., have triggered intense research activity in these multilayers. GMR sensors are not only very sensitive, but they can be made very small in size. For practical purposes, not only does one need large GMR, but also small saturation fields.

The aim of the present work is to study the temperature dependence of electrical resistivity and magnetoresistance in GMR multilayer stacks prepared by ion-beam sputter deposition. Typical multilayers reported here comprise 30 repeat layers of [Fe(20 Å)/Cr(10 Å)] that have been deposited by ion-beam sputter deposition onto Si substrates with xenon ions at 900 V and a beam current of 20 mA.

GMR in multilayers can be understood in terms of some simple ideas as follows. In zero magnetic field the ferromagnetic Fe layers are coupled antiferromagnetically through the Cr spacer layer, giving rise to a high electrical resistance. This antiferromagnetic (AF) coupling is ascribed to the indirect exchange interaction between the Fe layers through the oscillatory RKKY interaction mediated by the conduction electrons. The above antiferromagnetic coupling between Fe layers was established by means of light scattering from spin waves.[1] As the external field increases, the spins in different Fe layers align in the direction of the field, producing a completely ferromagnetic alignment beyond a saturation field H_{sat}, reducing the resistance. Thus we have a negative magnetoresistance (MR).

Magnetoresistance is defined (in textbook fashion) by

$$\mathrm{MR}=\frac{\rho(H,T)-\rho(0,T)}{\rho(0,T)}\times 100\%. \tag{1}$$

It is found in dc-magnetron-sputtered Fe-Cr superlattices[2] that GMR oscillates as a function of Cr spacer thickness with three gradually decreasing peaks centered at 11, 27, and 42 Å Cr for Fe thickness of 32 Å. Also, the first antiferromagnetic region occurs between 6 and 11 Å Cr for Fe thickness lying between 15 and 40 Å. We have therefore chosen the Cr thickness around 10 Å corresponding to the strongest peak of the antiferromagnetic coupling between the Fe layers (and hence the highest GMR).

The basic qualitative features of GMR can be understood even in terms of bulk scattering only if the mean free path (mfp) of electrons within the layers is much larger than the

layer thickness. If the mfp of the electrons is larger than the Cr spacer thickness, the electrons can feel the relative orientation of the magnetization of the successive layers. However, this interplay between the successive magnetic layers disappears and the GMR vanishes if the mfp is less than the Cr layer thickness.

GMR is attributed to the spin-dependent conduction properties of ferromagnetic metals. In a ferromagnetic metal or alloy the electrical conduction takes place through independent channels by spin-up (called majority) and spin-down (called minority) electrons. This is the two-current model of Fert and Campbell[3] whose physical basis is the dominance of the spin-conserving scattering and the weakness of the spin-flip collision, at least at low temperatures. In this picture all electrons of a given spin (up or down) with *s* or *d* or hybridized character are grouped together to form majority (up) or minority (down) bands. If one takes into account the details of the band structure of Fe (a weak ferromagnet) and the simple Drude conductivity formula for each band, it is easily shown[4] that the majority band has a much higher conductivity than the minority band. As a result, in the ferromagnetic alignment brought about by the saturation field ($H_{\rm sat}$), there is hardly any scattering for the majority-band electrons since they remain majority in all the Fe layers. On the other hand, the minority-band electrons get scattered within every Fe layer. Hence there is a short-circuiting effect, so to say, and the resistance ($\rho_{\rm FM}$) drops in the ferromagnetic alignment. However, in the antiferromagnetic configuration (zero field) both the majority and minority-band electrons are scattered in successive layers, and there is no short-circuiting effect. Therefore, the resistance ($\rho_{\rm AF}$) remains relatively high. A very simple calculation based on the two-current model shows that the GMR at low temperatures is given by (considering only bulk scattering)

$$\mathrm{GMR}=\frac{\rho(H=H_{\rm sat})-\rho(0)}{\rho(0)}=\frac{\rho_{\rm FM}-\rho_{\rm AF}}{\rho_{\rm AF}}=-\left(\frac{\rho_{\downarrow}/\rho_{\uparrow}-1}{\rho_{\downarrow}/\rho_{\uparrow}+1}\right)^2, \tag{2}$$

where $\rho_{\downarrow}$ and $\rho_{\uparrow}$ are the resistivities of the minority and majority carriers, respectively. It turns out that interface scattering from imperfect interfaces, defects, and impurities in Fe-Cr multilayers is also spin dependent and gives rise to the GMR. As a matter of fact, it is the imbalance between the resistivities of the two bands which is responsible for the GMR for bulk, interface, and spin-flip scattering. The subject of GMR has been reviewed very well in a recent book.[5]

Considerable work has been reported on the electrical transport and magnetic properties of Fe-Cr multilayers prepared by sputtering[2,6] or molecular-beam epitaxy (MBE).[6–8] The temperature dependence of the electrical resistivity in $[\mathrm{Fe}(30\,\text{Å})/\mathrm{Cr}(10-50\,\text{Å})]\times 10$ multilayers, prepared by sputtering and MBE, was interpreted by Almeida *et al.*[6] in terms of phonon-assisted *s*-*s* and *s*-*d* scattering in the temperature range of 15–300 K and in a saturation magnetic field of 7.5 kOe.

In the antiferromagnetic Fe-Cr superlattice, made by dc magnetron sputtering, the temperature-dependent magnetoresistance [defined as $\rho_M(T)=\rho(T,H=0)-\rho(T,H=H_{\rm sat})$] was found by Mattson *et al.*[2] to follow the equation for $T<100$ K:

$$\rho_M(T)=\rho_M(T=0)+\Delta\rho_M(T)=\rho_M(T=0)-aT^2, \tag{3}$$

where a is a constant of proportionality. This behavior was explained in terms of thermal excitation of magnons whose occupation number $(n)\propto T^2$ (at low temperatures) for anisotropic materials[9] and assuming $\Delta\rho_M(T)\sim n$.

In $[\mathrm{Fe}(12\,\text{Å})/\mathrm{Cr}(12\,\text{Å})]\times 10$ multilayers, prepared by MBE on MgO(100) substrates, several interesting observations were made by Aliev *et al.*[8] Among them are the following.

(a) The isothermal magnetoresistance, defined as $[\rho(0)-\rho(H)]$, is proportional to H in the parallel (magnetic field in the plane of the multilayers) orientation and to H^2 in the perpendicular case.

(b) A T-$H_{\rm sat}$ phase diagram was obtained, which clearly indicated the transition between AF and FM states.

(c) As opposed to the work of Mattson *et al.*[2] [which looked at the difference between the resistivity in the ideally antiferromagnetic ($H=0$) and ferromagnetic ($H=H_{\rm sat}$) alignments], here[8] the spin-dependent part of the electrical resistivity, defined as $\rho_s(T)=\rho(T,H)-\rho(T,H>H_{\rm sat})$ for fields $H\geqslant 0$ (where one has both ferromagnetic and antiferromagnetic fractions), is found to vary in a wide range of temperature below 100 K as

$$\rho_s(T)=\rho_s(T=0)+\Delta\rho_s(T)=b-cT^{\alpha}, \tag{4}$$

where $b=\rho_s(T=0)$ and the temperature exponent α are functions of the magnetic field H, and c is a constant of proportionality. The constant α was found[8] to be $\simeq 1.7$ for $H\simeq 0$, $\simeq 2.0$ for $H<0.5H_{\rm sat}$, and $\simeq 1$ for $H\simeq H_{\rm sat}$. This is in contrast to the value of $\alpha=2$ for $H=0$ (purely antiferromagnetic) in the work of Mattson *et al.*[2] [Eq. (3) above].

(d) $\Delta\rho_s(T)$ was found to vary linearly with temperature from 20 mK to about 1.5 K "which could be due to electron scattering on critical thermal spin fluctuations."[8]

All the work summarized above is mostly on MBE-grown Fe-Cr multilayers and those made by dc magnetron sputtering. Although the present work is on Fe-Cr multilayers prepared by ion-beam sputter deposition, we do not believe that the underlying physics depends in any significant way on differences in these deposition techniques.

II. EXPERIMENT

Fe-Cr multilayers were prepared by the ion-beam sputtering technique and characterized by transmission electron microscopy (TEM), atomic force microscopy (AFM), Auger electron spectroscopy (AES), and x-ray photoelectron spectroscopy (XPS), as well as resistivity, magnetic hysteresis loop, and magnetotransport measurements. The film deposition procedure and film properties, including chemical composition, surface morphology, resistivity, saturation magnetization, coercive field, and magnetoresistance ratio, are discussed in detail in Ref. 10. Values of GMR ratios of the films are comparable to values measured for polycrystalline

Fe-Cr films deposited by the more conventional rf sputtering technique.[11] We have deposited the following Fe-Cr multilayer combinations:

$$\mathrm{Si/Cr(50\,\text{Å})/[Fe(20\,\text{Å})/Cr(}t(\text{Å})\mathrm{)]}\times 30\mathrm{/Cr(50}-t(\text{Å})\mathrm{)},$$

where t was varied from 8 to 14 Å; this range surrounds the first antiferromagnetic maximum in the Fe-Cr multilayer system. The deposition rates varied from 5 to 30 Å/min depending on the primary ion-beam energy, the type of ions, and the target material. The films were deposited at room temperature. The effects of variations of the primary ion-beam energy and the type of ions on GMR values were examined; the investigated primary ion energy range was 700–1200 eV for Ar ions and 900–1200 eV for Xe ions. It was demonstrated that the GMR ratio is greater for films deposited using Xe ions than for films deposited using Ar ions, and that for both types of ions the GMR ratio increases as the primary ion-beam energy decreases. In this investigation we report the work on Fe-Cr multilayers of typical structure $[\mathrm{Fe}(20\,\text{Å})/\mathrm{Cr}(10\,\text{Å})]\times 30$ layers grown on Si substrates using Xe ions at 900 V and a beam current of 20 mA.

The temperature dependence of the resistance between 5 and 300 K of the Fe-Cr multilayers was measured in zero as well as in some applied magnetic fields using the standard four-probe dc technique and a magnetic field (0–5.5 T) provided by a Quantum Design superconducting quantum interference device (SQUID) magnetometer (MPMS). Both the transport current and applied field were in the plane of the film with the current parallel to the field. For measurements in magnetic fields perpendicular to the film plane we used a Quantum Design physical property measurement system (PPMS). We used the same MPMS to measure the magnetization of the Fe-Cr multilayers as a function of external fields at temperatures down to 2 K.

III. RESULTS AND DISCUSSION

Figure 1 shows the magnetoresistance versus external field H (kOe) for a typical Xe-ion-sputtered Fe-Cr multilayer sample at 10 and 300 K. The MR becomes constant at a saturation field H_{sat} (vertical arrow) around 13 kOe with typical values of 21% at 10 K. These values compare favorably with 30% and 40% obtained in dc-magnetron-sputtered and MBE-grown samples, respectively. Hysteresis in the MR was negligible as the magnetic field was swept from $(0\rightarrow 20\rightarrow 0\rightarrow -20\rightarrow 0)$ kOe.

A. Temperature dependence of the electrical resistivity

Figure 2 shows the electrical resistivity (ρ) versus temperature (T) for sample 1 at several values of the external magnetic field from 0 to 12 kOe. The saturation field (H_{sat}) has a weak temperature dependence; namely, it decreases with increasing temperature. This is clear from the $\rho(T)$ curves, say, at 10 and 12 kOe. They are closer to each other at higher temperatures.

To interpret the temperature dependence of the electrical resistivity, $\rho(T)$, at an intermediate field between $H=0$ and $H=H_{\mathrm{sat}}$ is not simple. In this magnetic field region the material has both antiferromagnetic and ferromagnetic fractions. Instead, for $H\geqslant H_{\mathrm{sat}}$, the alignment of the spins of each Fe layer is parallel to the direction of the external field, giving rise to a fully ferromagnetic state. It is well known in crystalline bulk $3d$ metals and alloys that the electron-phonon scattering contribution to the electrical resistivity from ρ_{sd} dominates over ρ_{ss} due to the overlap of the s and d bands at the Fermi level. Specifically, for Fe the density of states of the $3d^{\uparrow}$ majority band at the Fermi level is rather large compared to those of the s bands. The resistivity ρ_{sd} is given by the Bloch-Wilson formula.[12] The ''spin-disorder resistivity'' coming from the electron-magnon (spin-wave contribution) scattering is well described[13] by a relatively small term varying as T^2 in ferromagnets like Fe, Co, and Ni. Putting all these contributions together along with the residual resistivity ρ_0 one can write, assuming Mathiessen's rule

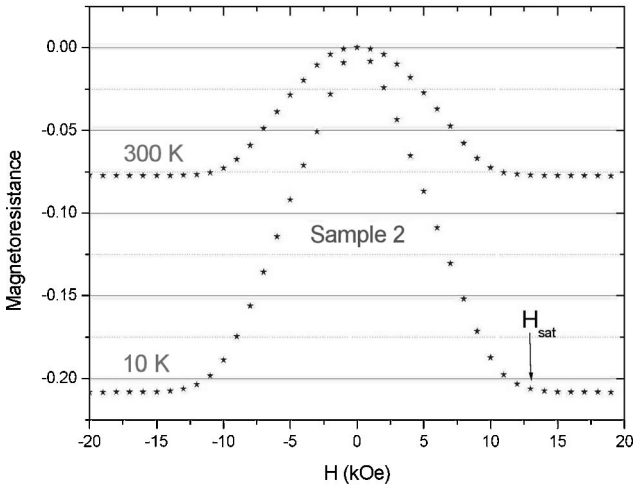

FIG. 1. Magnetoresistance vs external field H (kOe) oriented parallel to the layers for a Xe-ion-beam-sputtered Fe-Cr multilayer sample (sample 2) at 10 and 300 K. The MR saturates around 13 kOe (H_{sat}) and has a typical GMR of 21% at 10 K.

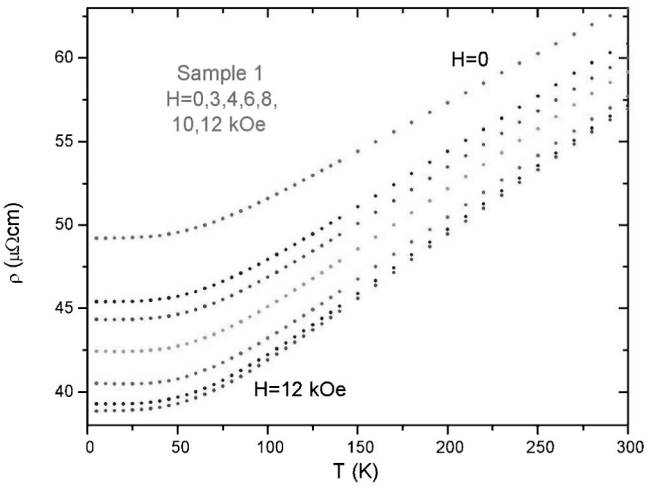

FIG. 2. Electrical resistivity (ρ) vs temperature (T) for sample 1 at several fields between 0 and 12 kOe. The curves are closer to each other at higher temperatures, indicating that the saturation field H_{sat} decreases with increasing temperature.

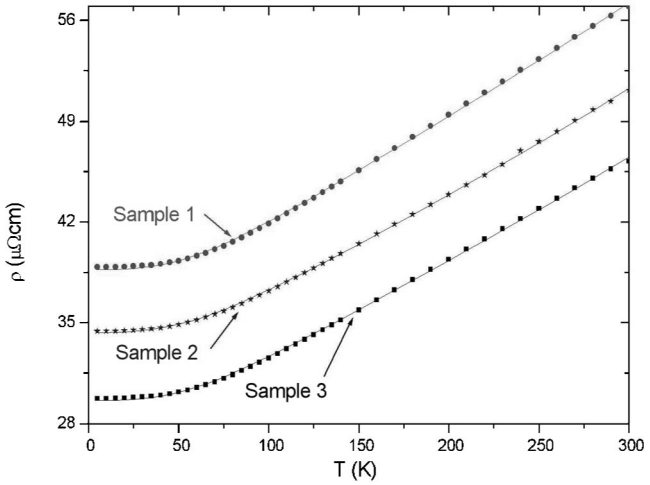

FIG. 3. Electrical resistivity (ρ) vs temperature (T) data (points) from 5 to 300 K for samples 1, 2, and 3 at their respective H_{sat}. The solid lines are the excellent least-squares fitted curves for fits to Eq. (5) which includes lattice and magnetic scattering contributions.

$$\rho(T,H=H_{\mathrm{sat}})=\rho_0+A\left(\frac{T}{\Theta_D}\right)^3\int_0^{\Theta_D/T}\frac{z^3dz}{(e^z-1)(1-e^{-z})}+BT^2, \tag{5}$$

where the second term is the Bloch-Wilson contribution ρ_{sd} and the third term is the small electron-magnon contribution increasing with temperature due to thermal excitation of magnons.

Taking the Debye temperature $\Theta_D=420\,\mathrm{K}$ for Fe-Cr multilayers,[6] we have fitted the data for five samples at their respective H_{sat} to Eq. (5) using a three-parameter least-squares fit program which also evaluated the integral numerically at each iteration. Excellent fits were obtained for all the samples with correlation coefficients of 0.999 995 and values of the normalized χ^2 consistent with the number of degrees of freedom and error estimates. Figure 3 shows ρ vs T data (points) for three samples from 5 to 300 K at their respective H_{sat}. The solid lines are the best-fit curves to Eq. (5). It is found that the value of the coefficient of the magnetic scattering term B averaged over all five samples is $(4\pm1)\times10^{-5}\,\mu\Omega\,\mathrm{cm\,K^{-2}}$ compared to $1.5\times10^{-5}\,\mu\Omega\,\mathrm{cm\,K^{-2}}$ in bulk ferromagnets (Fe, Co, Ni). This higher value of B may be related to the fact that the resistivity of these Fe-Cr multilayers at 300 K is about 5 times larger than that of bulk iron.

The fits of the data of Fig. 3 to Eq. (5) without the magnetic (BT^2) term are distinctly inferior to those with the magnetic term. The values of χ^2 are typically 6 times larger and the correlation coefficients poorer for the fits without the magnetic term. The deviation of the actual data from the best-fit values (residuals) is plotted in Fig. 4 as a function of temperature for sample 2 for both the fits. The deviation is much less ($<0.1\,\mu\Omega\,\mathrm{cm}$ in 40 $\mu\Omega\,\mathrm{cm}$) and more random for the fits with the magnetic term than without it. Addition of a Bloch-Grüneissen (BG) term (ρ_{ss}), which has a T^5 dependence, or replacing the Bloch-Wilson term by the BG term makes the fit much worse.

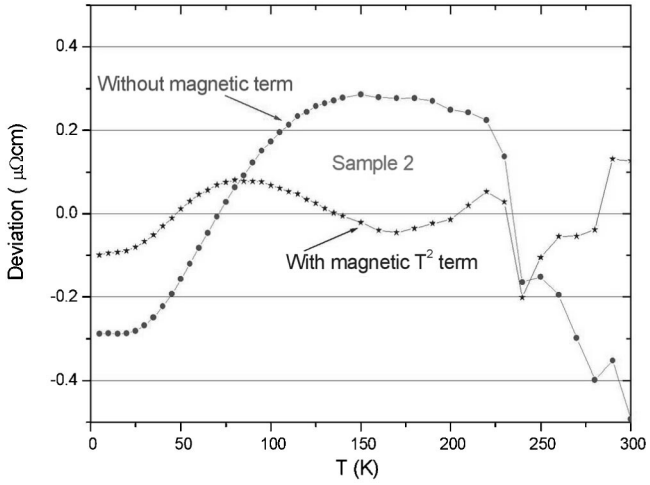

FIG. 4. The deviation of the actual data from the best-fit values is plotted as a function of temperature (T) for sample 2 for fits with and without the magnetic T^2 term. The deviation is much less (<0.1 $\mu\Omega\,\mathrm{cm}$ in 40 $\mu\Omega\,\mathrm{cm}$) and more random for the fits with the magnetic term than that without it.

B. Temperature dependence of the magnetoresistance

At $H=0$ these multilayers are ideally in an antiferromagnetic state where the neighboring ferromagnetic Fe layers are all antiferromagnetically coupled, resulting in a higher resistivity. Actually, there may be pinholes through the Cr spacer layer directly coupling the Fe layers ferromagnetically instead. Let us define an antiferromagnetic fraction (AFF) as

$$\mathrm{AFF}(H)=[1-M(H)/M_s]\times100\%, \tag{6}$$

where M_s is the magnetization measured at $H=H_{\mathrm{sat}}$ and $M(H)$ is the magnetization when the field is reduced from saturation to H, all at 5 K. Our $M(H)$ measurements on these samples show that the AFF is typically 80% at $H=0$. As H is increased, the Fe layers gradually turn their magnetization in the direction of the external field, reducing the AFF and hence the resistivity. Finally, the AFF reduces to zero (fully ferromagnetic alignment) and the resistivity and hence the GMR saturate at $H=H_{\mathrm{sat}}$.

We define $\Delta\rho(T)=\rho(T,H=0)_{\mathrm{AF}}-\rho(T,H=H_{\mathrm{sat}})_{\mathrm{FM}}$ as the difference in resistivity at a given temperature T between the AF ($H=0$) and the FM ($H=H_{\mathrm{sat}}$) states, both assumed ideal. This $\Delta\rho(T)$ is primarily due to the additional spin-dependent scattering (both bulk and interface) in the antiferromagnetic state. It is assumed here that the residual resistivity and the interband s-d scattering (dominant for $3d$ metals and alloys) do not depend strongly on magnetic fields. Figure 5 plots $\Delta\rho(T)$ vs T data (stars) for samples 1 and 3. Thus the additional spin-dependent scattering (resistivity) in the AF state decreases with increasing temperature. Just like the magnetic field aligns the spins in different Fe layers reducing the AFF (gradually bringing ferromagnetic order in its place) and produces a negative magnetoresistance, here temperature reduces the antiferromagnetic order (potentially bringing down the AFF) and hence $\Delta\rho(T)$. It is seen from Fig. 5 that $\Delta\rho$ varies as T^2 at low temperatures and is roughly linear at higher temperatures.

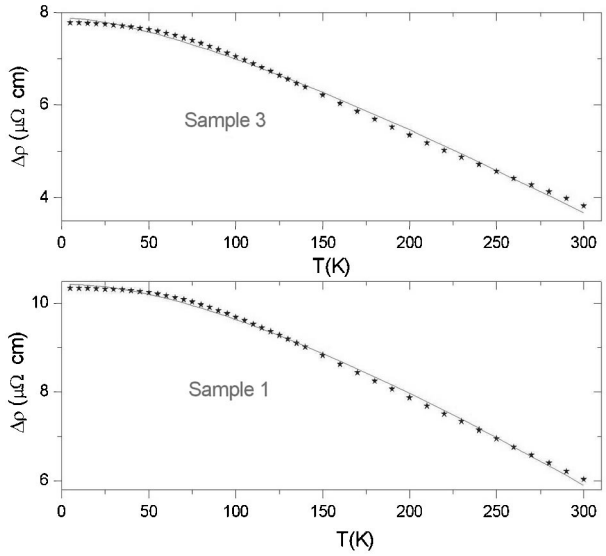

FIG. 5. $\Delta\rho(T)=\rho(T,H=0)_{\mathrm{AF}}-\rho(T,H=H_{\mathrm{sat}})_{\mathrm{FM}}$ vs temperature (T) data (stars) for samples 1 and 3. This additional spin-dependent resistivity in the AF state decreases with temperature. $\Delta\rho$ varies as T^2 at low temperatures and roughly linearly at higher temperatures. The solid lines are the least-squares fitted curves for fits to Eq. (7).

Singh *et al.*[9] had worked out the reduction in antiferromagnetic order due to thermal excitation of spin waves in highly anisotropic antiferromagnets with weak interlayer coupling between the antiferromagnetic planes. This theory has been extended in the present case where each Fe layer is ferromagnetic, but coupled antiferromagnetically to the neighboring Fe layers due to the RKKY interaction. In terms of the planar and interlayer exchange energies J_p and J_z, respectively, the sublattice magnetization $m(T)$ at temperature T is given in the Appendix [Eq. (A6)]. Assuming $\Delta\rho(T)\sim m(T)$, we have the relation

$$\frac{\Delta\rho(T)}{\Delta\rho(0)}=1-\frac{1}{\pi^2}\frac{T}{J_p}\int_0^{\pi/2}dq_z\ln\left(\frac{1}{1-e^{(-J_z/T)(1-\cos^2 q_z)^{1/2}}}\right), \tag{7}$$

where $m(0)=1$. The expression on the right differs only insignificantly from the corresponding expression for $m(T)/m(0)$ obtained earlier[9] for the anisotropic antiferromagnet ($\cos^2 q_z$ instead of $\cos q_z$), where it was shown to fall off as T^2 at low temperatures ($T\ll J_z$), crossing over to an approximately linear ($T\ln T$) fall off at high temperatures ($T\gg J_z$). We note that this expression is relatively unchanged when ferromagnetic domains are included.

We numerically evaluated the integral in Eq. (7) and used a three-parameter least-squares fit program to fit the data of Fig. 5. The resulting best-fit curves, shown by solid lines in Fig. 5, yield values of χ^2 consistent with the experimental errors and a correlation coefficient of 0.9999. Estimates of J_p and J_z are found from the above fits. They are (230 ± 20) K and (70 ± 20) K, respectively. The value for J_p is well below the Curie temperature (1040 K) for bulk iron, but could be closer to the unknown Curie temperature of 20-Å-thick Fe films sandwiched between Cr spacer layers. The value for J_z is, however, satisfying, close to the recently identified glass temperature, $T_g=140$ K, of an antiferromagnetic glassy phase that coexists with GMR in similar multilayer films. Irreversibilities in this glassy phase have been shown to arise from the same interlayer coupling that drives the antiparallel alignments in GMR.[14]

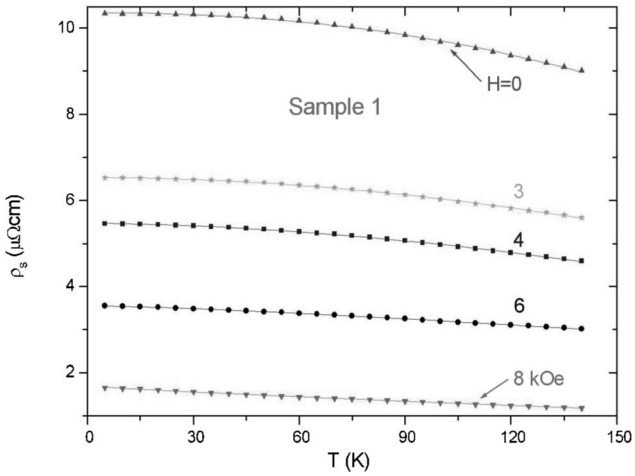

FIG. 6. $\rho_s(T)=\rho(T,H)-\rho(T,H_{\mathrm{sat}})$ vs temperature (T) data (points) for sample 1 at $H=0$, 3, 4, 6, and 8 kOe. The solid lines are the least-squares fitted curves for fits to Eq. (4).

Consistent with the above model are experimental data taken by us (not shown) and others[7] in which the saturation fields are studied as a function of spacer layer thickness. For three-ion-beam sputter-deposited ten-layer samples of Fe(20 Å)/Cr(d_{Cr}) with different Cr spacer layer thickness (d_{Cr}) we have observed that as d_{Cr} increases from 8 to 12 Å, the saturation field (H_{sat}) decreases from 10 to 5 kOe. As J_z decreases with increasing d_{Cr}, smaller external fields are necessary to break the antiferromagnetic coupling between the Fe layers.

C. Temperature dependence of the magnetoresistance in intermediate fields ($0\leqslant H\leqslant H_{\mathrm{sat}}$)

Following the work of Aliev *et al.*,[8] we have fitted our data for samples 1, 2, and 3 to Eq. (4) with $\rho_s(T)=\rho(T,H)-\rho(T,H_{\mathrm{sat}})$. The data points along with the least-squares fit curves are shown in Fig. 6 for sample 1 for $H=0$, 3, 4, 6, and 8 kOe. Excellent fits are obtained for all the samples with values of χ^2 consistent with the experimental error, correlation coefficients $R^2\simeq0.999$, and small errors in the fitting parameters b, c, and α. The fits are, however, better for smaller fields. Figure 7 shows α of Eq. (4) vs H/H_{sat} for all the three samples. The solid lines are just guides to the eye. The shape of the curve is rather similar to the results obtained by Aliev *et al.*[8] (summarized at the end of the Introduction and Fig. 3 of Ref. 8) for MBE-grown samples. However, we find some differences, like α in our work being typically 2 for $H/H_{\mathrm{sat}}<1/3$, becoming $\simeq1$ for $H/H_{\mathrm{sat}}\simeq2/3$, and decreasing at still higher fields. This implies that ρ_s vs T curves (Fig. 6) are quadratic in lower fields and linear around $H/H_{\mathrm{sat}}\simeq2/3$ instead of $\simeq1$ as in the work of Aliev *et al.*[8]

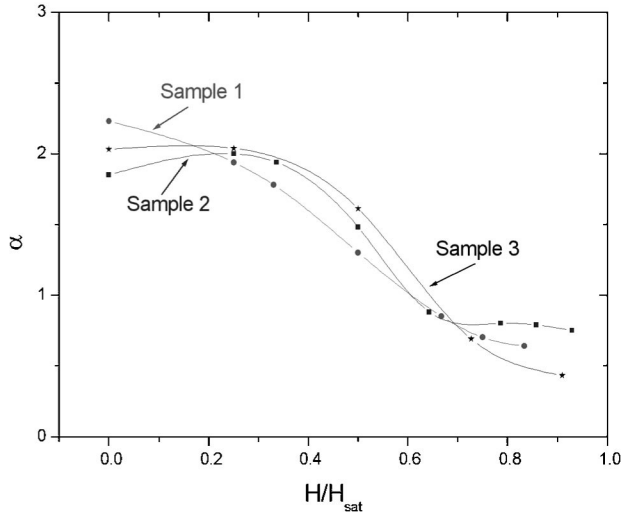

FIG. 7. α of Eq. (4) vs H/H_{sat} for all the three samples. The solid lines are just guides to the eye.

It is found from Fig. 6 that the intercept b decreases with increasing applied fields. This is simply due to the fact that the antiferromagnetic fraction decreases with increasing field. If we plot b as a function of our measured values of AFF (%) for samples 1 and 3, we find, as shown in Fig. 8, that b increases with the AFF in a monotonic fashion (both decreasing with H). This is a logical conclusion since as $H \rightarrow 0$, the AFF attains its maximum value giving the highest resistivity in the ideally AF ground state. It is to be noted that the decrease of b with H and the decrease of $\Delta\rho$ with T (Fig. 5) have a common origin. It is the decrease of the AFF brought about by H and T, respectively.

D. T vs H_{sat} phase diagram for the AF-FM transition

Figure 9 shows the low-field magnetoresistance of sample 4 (argon-ion sputtered) vs external field H for the parallel orientation (H in the film plane). It is amply clear that the

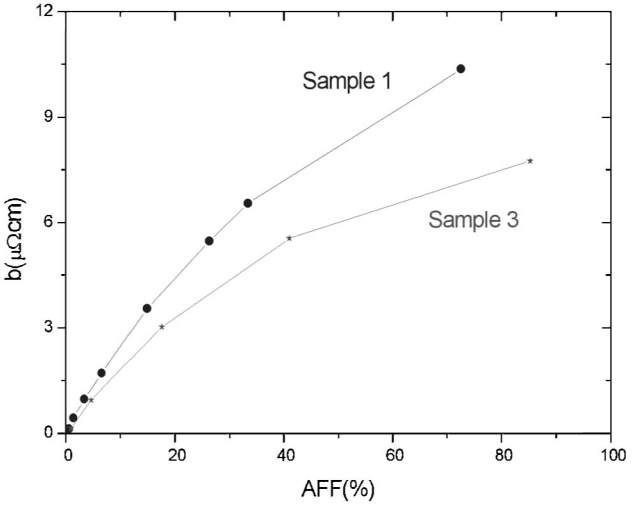

FIG. 8. b of Eq. (4) vs AFF(%) for samples 1 and 3. b is found to increase monotonically with the AFF (both increasing with H).

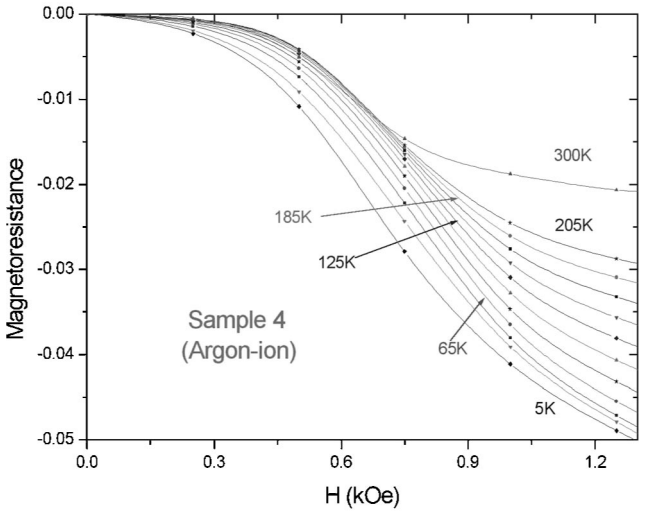

FIG. 9. Magnetoresistance vs external field H (kOe) at low fields for sample 4 (Ar-ion sputtered) for the parallel orientation (H in the film plane). The temperatures are between 5 and 205 K (every 20 K) and 300 K. Clearly, the MR$\sim H^2$ at lower fields.

MR$\sim H^2$ in contrast to the findings of Aliev *et al.*[8] [Fig. 1(a) of Ref. 8] who found that the MR is linear in H for their MBE-grown samples. We found no linear region in the MR vs H curve even at higher fields until the saturation field (H_{sat}) of 2–3 kOe was reached. As a matter of fact, sample 4 (Fig. 9) reflects an S-shaped curve, having points of inflection. However, for the perpendicular orientation (H perpendicular to the film plane) we find that the MR again goes as H^2, in agreement with the findings of Aliev *et al.*[8]

The observed H^2 dependence at low external fields is, in fact, expected from simple energy considerations, as argued below. The antiferromagnetic ground state of the multilayer is characterized by the sublattice magnetization $\mathbf{m}=(\mathbf{m}_A - \mathbf{m}_B)/2$, which takes into account the antiparallel orientation of the spin polarization in alternating Fe layers A and B. The direction of $\mathbf{m}$ is arbitrary in the ideal isotropic situation. When a small in-plane magnetic field is applied, the sublattice magnetization $\mathbf{m}$ aligns itself perpendicular to the direction of the field. This is the lowest-energy configuration as it allows for energy gain in all Fe layers due to twisting of spins in the field direction. If the twist angle is θ, assumed small, then the energy gain is $mH \sin\theta \approx mH\theta$. The twisting also costs energy $J_z m^2(1-\cos 2\theta) \approx 2J_z m^2\theta^2$ due to loss of antiferromagnetic exchange energy at the layer interfaces. Minimizing the net energy change yields the optimum twist angle $\theta(H)=H/4Jm$ as proportional to the field. Now the reduction in the sublattice magnetization or the antiferromagnetic fraction, and therefore the decrease in resistivity, due to this twist is $m[1-\cos\theta(H)]$, which goes as H^2 for low fields.

Figure 10 shows the T vs H_{sat} phase diagram for sample 4 (argon-ion sputtered, same as that of Fig. 9) and sample 1 (xenon-ion sputtered). Both are in parallel orientations. Here $H_{sat}(T)$ is the field at which the MR becomes field independent: i.e., the field-induced AF-to-FM transition is complete. The values of $H_{sat}(T=0)$ are $\simeq 3$ kOe for sample 4 and

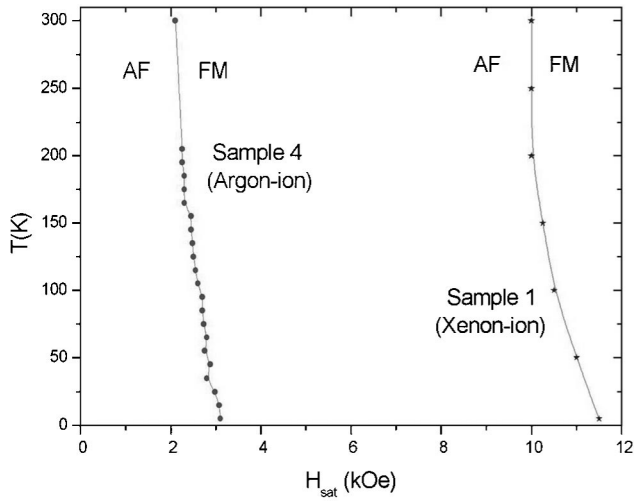

FIG. 10. T vs H_{sat} phase diagram for samples 4 (Ar-ion sputtered) and 1 (Xe-ion sputtered). Here H_{sat} is the field at which the MR becomes field independent; i.e., the field-induced AF-to-FM transition is complete. The values of $H_{sat}(T=0)$ are 3 kOe for sample 4 and 11.5 kOe for sample 1.

$\simeq$11.5 kOe for sample 1. Figure 10 is very similar to Fig. 1(b) of Ref. 8 on MBE-grown samples for the parallel orientation.

IV. CONCLUSIONS

The temperature dependence of the electrical resistivity and magnetoresistance has been studied in ion-beam-sputtered Fe-Cr multilayers. Typical in-plane negative giant magnetoresistance is 21% at 10 K saturating at around 1 T. Here each Fe layer is ferromagnetic but coupled antiferromagnetically in zero field to the neighboring Fe layers due to the RKKY interaction. This gives rise to a high resistance. An external magnetic field aligns the spins in different Fe layers producing a ferromagnetic alignment beyond H_{sat} which reduces the electrical resistance. The electrical resistivity in the fully ferromagnetic state ($H=H_{sat}$) between 5 and 300 K has been interpreted as the sum of a residual resistivity, electron-phonon *s-d* scattering, and spin-disorder resistivity [Eq. (5)]. The latter has the same order of magnitude as in crystalline Fe.

We have calculated the sublattice magnetization $m(T)$ of these Fe-Cr multilayers in terms of the planar and interlayer exchange energies [Eq. (A6) of the Appendix]. The additional spin-dependent scattering in the antiferromagnetic state at $H=0$, defined by $\Delta\rho(T)=\rho(T,H=0)_{AF}-\rho(T,H=H_{sat})_{FM}$, is obtained from the experimental data by assuming that the residual resistivity and the electron-phonon scattering are roughly independent of the field. The decrease in $\Delta\rho(T)$ with increasing temperature from 5 to 300 K is explained as arising from the reduction in the antiferromagnetic order due to the thermal excitation of spin waves, i.e., $\Delta\rho(T)\sim m(T)$. Mattson *et al.*,[2] on the other hand, in dc-magnetron-sputtered Fe-Cr superlattice, found $\Delta\rho(T)$ decreasing as T^2 at temperature below 100 K [Eq. (3)] in contrast to our fits [Eq. (7)] over a much wider temperature range.

From our data at intermediate fields ($0<H<H_{sat}$), the spin-dependent part of the electrical resistivity, defined as $\rho_s(T)=\rho(T,H)-\rho(T,H>H_{sat})$, fits very well to Eq. (4). We find that α is typically 2 for $H/H_{sat}<1/3$, becoming ~ 1 for $H/H_{sat}\simeq 2/3$, and then decreasing further at still higher fields. The decrease of the intercept b with increasing H and that of $\Delta\rho(T)$ with increasing T [Eq. (7)] are due to the decrease of the antiferromagnetic fraction [Eq. (6)] with increasing H and T, respectively. Very similar conclusions were reached by Aliev *et al.*[8] in MBE-grown Fe-Cr multilayers.

Finally, we have also obtained the T-vs-H_{sat} phase diagram for the field-induced AF-to-FM transition.

ACKNOWLEDGMENTS

One of us (A.K.M.) acknowledges the Physics Department, University of Florida, Gainesville for local hospitality and experimental facilities. In addition, discussions with S. B. Arnason and S. Hershfield are gratefully acknowledged. This research was supported by a DOD/AFOSR MURI grant (No. F49620-96-1-0026).

APPENDIX

To obtain the magnon energies in the multilayer system, the following simplified Hubbard model is considered on a three-dimensional lattice consisting of a stack of layers in the z direction:

$$H=\sum_{\mathbf{k}\sigma}\epsilon_p(\mathbf{k})c^\dagger_{\mathbf{k}\sigma}c_{\mathbf{k}\sigma}-t_z\sum_{i\sigma}c^\dagger_{i\sigma}(c_{i+\delta,\sigma}+c_{i-\delta,\sigma}) + U\sum_i n_{n\uparrow}n_{i\downarrow}. \tag{A1}$$

Here the planar band energy $\epsilon_p(k_x,k_y)$ together with the correlation term describes the ferromagnetic layers, while the interlayer hopping term t_z, which connects sites i to nearest-neighbor sites $i\pm\delta$ in the neighboring layers, represents the AF exchange coupling between layers. We divide the multilayer system into two sublattices with alternating A and B layers, and consider a ground state in which the A layers have spin polarization $\langle n_i^\uparrow-n_i^\downarrow\rangle=+m$ in the $+z$ direction, while B layers have spin polarization $\langle n_i^\uparrow-n_i^\downarrow\rangle=-m$ in the $-z$ direction. The sublattice magnetization m, a dimensionless quantity, measures the AF order parameter in the multilayer system.

In this two-sublattice basis and in the Hartree-Fock (HF) approximation, the Hamiltonian reduces to

$$H=\sum_{\mathbf{k}\sigma}(a^\dagger_{\mathbf{k}\sigma}\ b^\dagger_{\mathbf{k}\sigma})\begin{bmatrix}\epsilon_p(\mathbf{k})-\sigma\Delta & \epsilon_z(\mathbf{k})\\ \epsilon_z(\mathbf{k}) & \epsilon_p(\mathbf{k})+\sigma\Delta\end{bmatrix}\begin{pmatrix}a_{\mathbf{k}\sigma}\\ b_{\mathbf{k}\sigma}\end{pmatrix}, \tag{A2}$$

where $a_{\mathbf{k}}$ and $b_{\mathbf{k}}$ are the Fourier transforms of the electronic annihilation operator c_i, defined on the two sublattices A and B, respectively. Here $2\Delta=mU$ and the sublattice magnetiza-

tion m is determined self-consistently. For simplicity we consider the strong correlation limit in which at the HF level $m \approx 1$. The interlayer band energy $\epsilon_z(\mathbf{k}) = -2t_z \cos k_z$ mixes the two ferromagnetic bands, and hence the quasiparticle band energies $E(\mathbf{k}) = \epsilon_p(\mathbf{k}) \pm \sqrt{\Delta^2 + \epsilon_z(\mathbf{k})^2}$ have a mixed character with features of both the ferromagnetic[15] and antiferromagnetic ground states.[16] As the planar (ferromagnetic) band energy $\epsilon_p(\mathbf{k})$ appears on the diagonal, the eigenvectors of the Hamiltonian matrix in Eq. (A2) are unchanged from the AF case.[16]

Evaluation of the magnon propagator $\chi^{-+}(\mathbf{q}\omega)$, involving transverse spin operators (S^-, S^+) and representing transverse spin fluctuations about the Hartree-Fock ordered state, has been described earlier in the random phase approximation (RPA) for both ferromagnetic[15] and antiferromagnetic[16] ground states. For the multilayer system the magnon propagator is obtained as

$$\chi^{-+}(\mathbf{q}\omega) = \begin{bmatrix} J_z + J_p q_p^2 - \omega & -J_z \cos q_z \\ -J_z \cos q_z & J_z + J_p q_p^2 + \omega \end{bmatrix} \frac{1}{\omega_{\mathbf{q}}^2 - \omega^2}, \tag{A3}$$

for small planar momentum $\mathbf{q_p} = (q_x, q_y)$. Here $J_z = 2t_z^2/\Delta \approx 4t_z^2/U$ is the exchange energy characterizing the antiferromagnetic coupling between layers, and J_p, the magnitude of which depends on details of the planar band energy $\epsilon_p(\mathbf{k})$, plays the role of the planar exchange energy. The magnon energy $\omega_{\mathbf{q}}$ is given by

$$\omega_{\mathbf{q}}^2 = (J_p q_p^2 + J_z)^2 - J_z^2 \cos^2 q_z, \tag{A4}$$

which has the right limiting behavior yielding the antiferromagnetic magnon energy $J_z\sqrt{1-\cos^2 q_z}$ as $J_p \to 0$ and the ferromagnetic magnon energy $J_p q_p^2$ as $J_z \to 0$. A completely different starting point in terms of a Heisenberg spin model for the multilayer system, with planar and interlayer exchange energies J_p and J_z, would yield the same result.

Going over now to the thermal excitation of magnons in the multilayer system, the change $\delta m(T) \equiv m(T) - m(0)$ in the sublattice magnetization at finite temperature T is obtained by considering both the advanced and retarded modes in the spin-fluctuation propagator with appropriate Bose weights. After subtracting out the zero-temperature (quantum fluctuation) part the reduction in the sublattice magnetization is obtained as

$$-\delta m(T) = \int_0^\infty \frac{2\pi q_p dq_p}{(2\pi)^2} \int_{-\pi}^{\pi} \frac{dq_z}{2\pi} \frac{J_z + J_p q_p^2}{\omega_{\mathbf{q}}} \frac{2}{e^{\beta\omega_{\mathbf{q}}} - 1}. \tag{A5}$$

Here the upper limit of integration for the q_p integral has been taken as ∞ for convenience, which is valid at temperatures low compared to J_p, as the high-energy modes have exponentially small weight. Integration over the planar momentum q_p finally yields

$$m(T) = m(0) - \frac{1}{\pi^2} \frac{T}{J_p} \int_0^{\pi/2} dq_z \ln\left[\frac{1}{1 - e^{(-J_z/T)(1-\cos^2 q_z)^{1/2}}}\right]. \tag{A6}$$

*Author to whom correspondence should be addressed. Electronic address: akm@iitk.ac.in

[1] P. Grünberg, R. Schreiber, Y. Pang, M. B. Brodsky, and H. Sowers, Phys. Rev. Lett. **57**, 2442 (1986).
[2] J. E. Mattson, Mary E. Brubaker, C. H. Sowers, M. Conover, Z. Qiu, and S. D. Bader, Phys. Rev. B **44**, 9378 (1991).
[3] A. Fert and I. A. Campbell, J. Phys. F. Met. Phys. **6**, 849 (1976).
[4] P. B. Visscher and Hui Zhang, Phys. Rev. B **48**, 6672 (1993).
[5] *Magnetic Multilayers and Giant Magnetoresistance: Fundamentals and Industrial Applications*, edited by Uwe Hatmann, Springer Series in Surface Sciences, Vol. 37 (Springer, Berlin, 1999).
[6] B. G. Almeida, V. S. Amaral, J. B. Sousa, R. Colino, I. K. Schuller, V. V. Moschalkov, and Y. Bruynseraede, J. Appl. Phys. **85**, 4433 (1999).
[7] M. N. Baibich, J. M. Broto, A. Fert, F. Nguyen Van Dau, F. Petroff, P. Etienne, G. Creuzet, A. Friederich, and J. Chazelas, Phys. Rev. Lett. **61**, 2472 (1988).
[8] F. G. Aliev, V. V. Moshchalkov, and Y. Bruynseraede, Phys. Rev. Lett. **81**, 5884 (1998).
[9] A. Singh, Z. Tešanović, H. Tang, G. Xiao, C. L. Chien, and J. C. Walker, Phys. Rev. Lett. **64**, 2571 (1990).
[10] J. M. Lannon, Jr., D. Temple, G. E. McGuire, C. C. Pace, and A. F. Hebard (unpublished).
[11] S. S. P. Parkin, N. More, and K. P. Roche, Phys. Rev. Lett. **64**, 2304 (1990).
[12] A. G. Wilson, Proc. R. Soc. London, Ser. A **167**, 580 (1938).
[13] D. A. Goodings, Phys. Rev. **132**, 542 (1963).
[14] N. Theodoropoulou, A. F. Hebard, M. Gabay, A. K. Majumdar, C. Pace, J. Lannon, and D. Temple (unpublished).
[15] S. Doniach and E. H. Sondheimer, *Green's Functions for Solid State Physicists* (Benjamin, New York, 1974).
[16] A. Singh and Z. Tešanović, Phys. Rev. B **41**, 614 (1990); **41**, 11 457 (1990).